



HAL
open science

Polymorphism of Two-Dimensional Halogen Bonded Supramolecular Networks on a Graphene/Iridium(111) Surface

Muriel Sicot, Damien Tristant, Iann Gerber, Bertrand Kierren, Frédéric Chérioux, Yannick Fagot-Revurat, Luc Moreau, Julien Granet, Daniel Malterre

► **To cite this version:**

Muriel Sicot, Damien Tristant, Iann Gerber, Bertrand Kierren, Frédéric Chérioux, et al.. Polymorphism of Two-Dimensional Halogen Bonded Supramolecular Networks on a Graphene/Iridium(111) Surface. *Journal of Physical Chemistry C*, 2017, 121 (4), pp.2201-2210. 10.1021/acs.jpcc.6b09892 . hal-01961179

HAL Id: hal-01961179

<https://hal.insa-toulouse.fr/hal-01961179>

Submitted on 16 May 2019

HAL is a multi-disciplinary open access archive for the deposit and dissemination of scientific research documents, whether they are published or not. The documents may come from teaching and research institutions in France or abroad, or from public or private research centers.

L'archive ouverte pluridisciplinaire **HAL**, est destinée au dépôt et à la diffusion de documents scientifiques de niveau recherche, publiés ou non, émanant des établissements d'enseignement et de recherche français ou étrangers, des laboratoires publics ou privés.

Polymorphism of 2D Halogen Bonded Supramolecular Networks on a Graphene/Iridium(111) Surface

Muriel Sicot,^{*,†} Damien Tristant,^{‡,¶} Iann C. Gerber,[‡] Bertrand Kierren,[†] Frédéric Chérioux,[§] Yannick Fagot-Revurat,[†] Luc Moreau,[†] Julien Granet,[†] and Daniel Malterre[†]

[†]*Institut Jean Lamour, UMR 7198, CNRS Université de Lorraine, BP 70239, 54506 Vandoeuvre lès Nancy, France*

[‡]*Université de Toulouse, INSA-CNRS-UPS, LPCNO, 135 Avenue de Rangueil, 31077 Toulouse, France*

[¶]*CEMES, UPR 8011, CNRS-Université de Toulouse, 29 rue Jeanne Marvig, BP 94347, 31055 Toulouse, France*

[§]*Institut FEMTO-ST, Université de Bourgogne Franche Comté, CNRS, 15B Avenue des Montboucons, F-25030 Besançon cedex, France*

E-mail: muriel.sicot@univ-lorraine.fr

Abstract

The properties of 2D supramolecular self-assemblies on surfaces depend on the fine balance between molecule-substrate and molecule-molecule interactions. In this article, we study the growth of 1,3,5-tri(4'-bromophenyl)benzene (TBB) monolayer on graphene epitaxially grown on Ir(111) by means of low temperature scanning tunneling microscopy and spectroscopy (LT-STM/STS) combined with a fully atomistic

description of the molecules in interaction with the Gr/Ir(111) substrate, using density functional theory (DFT). In order to figure out the impact of the underlying metallic layer upon the self-assembling behavior of the molecules and their properties, we compare our results with those theoretically obtained on pristine graphene or experimentally achieved on HOPG. We demonstrated that the use of the Ir layer allows the formation of large extended, continuous and two-dimensional supramolecular networks laying even over Ir step edges like a carpet. In addition, we highlighted the obtention of two structural polymorphs never observed on HOPG. In the light of DFT simulations, we assumed that the formation of these polymorphs is driven by the balance between molecule-molecule interactions, due to Halogen bonds (XB), and the tailored molecule-surface interactions due to the presence of Ir layer.

Introduction

Molecular self-assembly is the spontaneous association of molecules into structurally stable well-defined aggregates joined by noncovalent interactions. This key concept allows for the engineering of molecular architectures with novel or targeted optical, electrical and magnetic properties. In supramolecular assembly, molecular building blocks are interconnected to each other by virtue of directional intermolecular interactions such as halogen bonding,¹ hydrogen bonding,^{2,3} dipolar coupling,^{4,5} metal coordination,⁶⁻⁸ van der Waals forces⁹⁻¹¹ or π - π interactions.¹² Nevertheless, on a surface, the resulting molecular geometry does not depend only on intermolecular interactions but on a subtle balance between molecule-molecule and molecule-substrate interactions. Therefore, opting for the right combination composed of a molecular building unit and a substrate would lead to the desired functional nanomaterial. Moreover, tunability could be obtained by the subtle modifications of the substrate properties.

In this framework, epitaxial graphene on metal (Gr/M) has emerged as an appealing support for molecular self-assembly.¹³ First, the presence of a moiré nanopattern¹⁴⁻¹⁷ originating from a lattice mismatch between the metal and the carbon layer leads to an interesting ad-

sorption energy landscape that can be exploited to grow novel molecular architectures such as nanoporous¹⁸ or Kagomé networks¹⁹ that could not be achieved using HOPG^{20,21} or other substrates. In addition, the coupling between Gr and the metal is an extra parameter to play with in order to modify the molecule-substrate interaction and therefore to obtain various and original molecular arrangements. For example, the growth of iron-phthalocyanine on Gr/Ru for which the carbon-metal interaction is strong leads to a Kagomé lattice whereas same molecules form densely packed 2D islands on Gr/Pt for which the coupling is weak.²²

Moreover, the advantage of using Gr/M substrates relies on the fact that even more complex Gr/X/M interfaces can be built for fine adsorption tuning by means of controlled intercalation of a foreign species X (atoms or molecules) between the graphene layer and the metallic support.²³⁻³⁰ Once again, the primary objective behind this interface engineering is to finely tune the electronic properties of the topmost graphene layer in order to have control on the resulting molecule-substrate interaction. In this vein, the possibility to manipulate molecular adsorption at the nanometer scale and to tailor molecular self-assembly using intercalation has been recently demonstrated.^{31,32} Finally, the growth of epitaxial graphene is carpet-like such that the carbon layer continuously covers the metallic step edges.^{29,33,34} Hence, unlike any other substrate, one could expect to avoid the disruption of the molecular network and therefore, obtain low-defect interface for graphene-based organic electronic devices with high performances.

Although HOPG has been widely used for molecular self-assembly, there is no straightforward way to deduce from these existing studies the self-assembly behavior on Gr/M since the interaction of graphene with the underlying layers (carbon in the case of HOPG and metal in the case of Gr/M) plays an important role in the number and nature of phases even in the case of weakly coupled Gr/M interfaces.^{20-22,35} Therefore, in order to understand how molecular properties can be affected by the substrate, it is crucial to determine the impact of the underlying metal layer below graphene on the self-assembly.

Here, we investigate by means of LT-STM/STS and DFT the structural and electronic

properties of self-assembly of 1,3,5-tri(4'-bromophenyl)benzene (TBB) molecules on Gr/Ir(111). The particular choice of this molecule is motivated by the fact that it can form self-assembly driven by halogen···halogen bonding on various substrates.³⁶⁻³⁸ Moreover, halogen bonded molecular self-assembly on Gr/M substrates are lacking. As this molecule has been previously investigated on semi-conducting,³⁹ metallic^{37,40-42} or graphite (HOPG) substrates,³⁷ a direct comparison with our results allows us to elucidate the role of the Gr/Ir interface in the assembly process. In this work, we demonstrate by LT-STM, the formation of a supramolecular carpet of high structural quality on Gr/Ir. In addition, the coexistence of two polymorphs is observed. We show that the two phases are composed of TBB dimers stabilized by Br···Br and Br···H bonds. The two polymorphs have been determined to be different than the single one previously obtained on HOPG³⁷ revealing the crucial role of the layer lying under the topmost graphene sheet. DFT demonstrates that the Ir has only little influence on the adsorption geometry of the molecule. However, LT-STS and simulated PDOS reveal that Ir acts on the energies of the HOMO and LUMO states of the adsorbed molecule via charge transfer with graphene. Finally, the comparison of our results with previous works shows that the use of Gr/Ir(111) results in original packings with unique electronic properties.

Results and discussion

System

The substrate is made of one single monolayer of graphene epitaxially grown on Ir(111) and prepared as described elsewhere.³⁰ At the sample scale (about one square centimeter), low-energy electron diffraction (LEED) patterns (not shown here) reveal a long-range ordered and single-domain graphene overlayer. A moiré superstructure resulting from a mismatch between graphene and Ir(111) lattices is also observed both with LEED and scanning tunneling microscopy (STM) (Fig. 1(a)) with a superperiodicity of about 2.5 nm corresponding

to approximately 10 times of the lattice constant of graphene and 9 times that of Ir(111). This is in good agreement with earlier works.¹⁵ As shown in Fig.1(b), this graphene corrugation is responsible for the creation of three regions for possible preferential molecular adsorption: FCC-, HCP-and ATOP-type. They are named for whether the center of the carbon hexagons sites above an Ir fcc-, hcp-hollow or atop site (up triangle, down triangle and circles circumscribe these regions in Fig. 1(b)). Fig. 1(c) displays a high-resolution STM topograph showing the graphene overlayer that spreads across an Ir step without visible defect at the atomic scale. This carpet-like growth has already been described by Coraux *et al.*³³ As we will show later on, this particular structural property is a key feature to obtain low defect density 2D self-assembled molecular networks (SAMNs). Indeed, this property to cover the Ir edge might lead to a reduction of the Ehrlich-Schwöbel barrier and therefore promote step edge crossing of the molecules during diffusion in comparison with diffusion on uncovered metallic surfaces such as Ag, Au. The TBB molecule is star shaped (Fig. 1(d)) and possesses a bromophenyl group at the extremity of its arms. In the gas-phase, a single molecule is not flat : each arm is rotated by a dihedral angle δ of about 39° between the phenyl groups and the central ring as obtained by gas-phase DFT optimization of the molecule and shown in Fig. 1(d)(bottom view) (see the computational details section below).

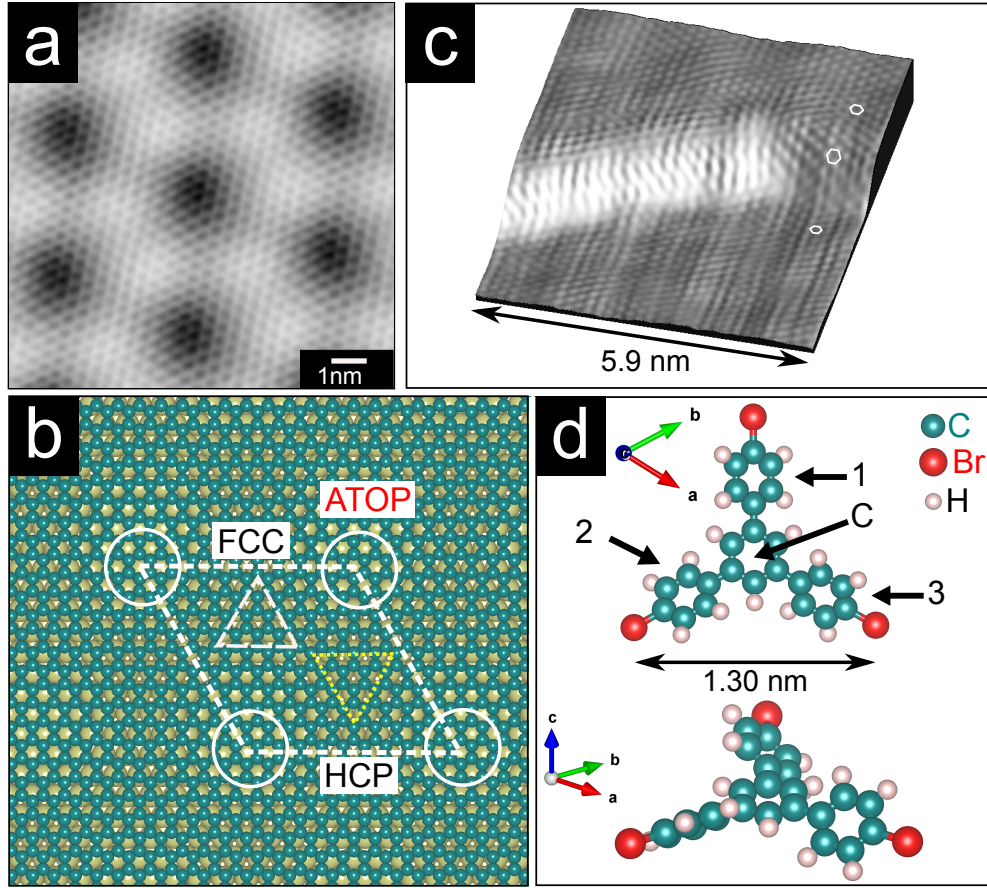


Figure 1: (a) Atomically-resolved STM topograph of the moiré structure of the graphene layer on Ir(111) ($U_T = 0.15$ V; $I_T = 2$ nA). (b) Schematic illustration of the DFT optimized C(10×10)/Ir(9×9) unit cell. Carbon and Ir atoms are represented as green and yellow spheres respectively. The dashed white rhombus outlines the supercell of the moiré superstructure with three different regions marked by a full circle (ATOP), an dashed up-pointing triangle (FCC) and a dotted down-pointing triangle (HCP) (see text). (c) 3D rendering of an atomically-resolved STM topograph showing the continuity of the graphene film across an Ir step edge. Three white hexagons schematically represent sp^2 bonds of the graphene film adsorbed on the upper, lower terraces and on the Ir step edge. (17×11 nm², $U_T = 9$ mV; $I_T = 12$ nA). (d) ball-and-stick model of the 1,3,5-tri(4'-bromophenyl)benzene (TBB) molecule in gaseous phase. Top: top view showing the three bromophenyl arms labeled 1,2 and 3 and the central benzene ring labeled C. Bottom: side view showing the dihedral rotation of the side groups.

Growth

The growth of TBB on Gr/Ir has been investigated in the submonolayer range. At early stages of growth, molecules adsorbed on the lower terraces along the Gr/Ir step edges as

shown in Fig. 2(a). At increasing coverages, TBB molecules self-assemble starting from the Gr/Ir step edges and form one molecule thick nanoislands as pointed by a white arrow in Fig. 2(b). Large defects on terraces can anchor molecules and act as starting points for molecules to self-assemble as well. Fig. 2(c) displays an STM topograph of a 2D SAMN of TBB molecules that spontaneously formed at higher coverage. Molecular patches as large as 200 nm were observed by means of STM. Two different polymorphs, labeled 2MOL and 4MOL in the following, were identified (Fig. 2(c) and (d)). Their respective occurrence and molecular packing will be discussed in details later in the text. White parallel lines in Fig. 2(c) outline one main crystallographic direction of the first polymorph. Those lines are not deviated when crossing the Gr/Ir step edge displayed as a vertical black line according to the color scale in the center of the STM image. This shows the continuity of the SAMN over the step edge. This feature can be easily understood considering the carpet-like growth of the graphene film on Ir as mentioned earlier: molecules adsorbed at any places on graphene independently of the vertical graphene lattice bending caused by the presence of Ir step edge. This feature is also well illustrated for the second polymorph in the 3D rendering of an STM topograph in Fig. 2(d) where the molecular network smoothly adopts the graphene deformation when crossing the Ir step edge.

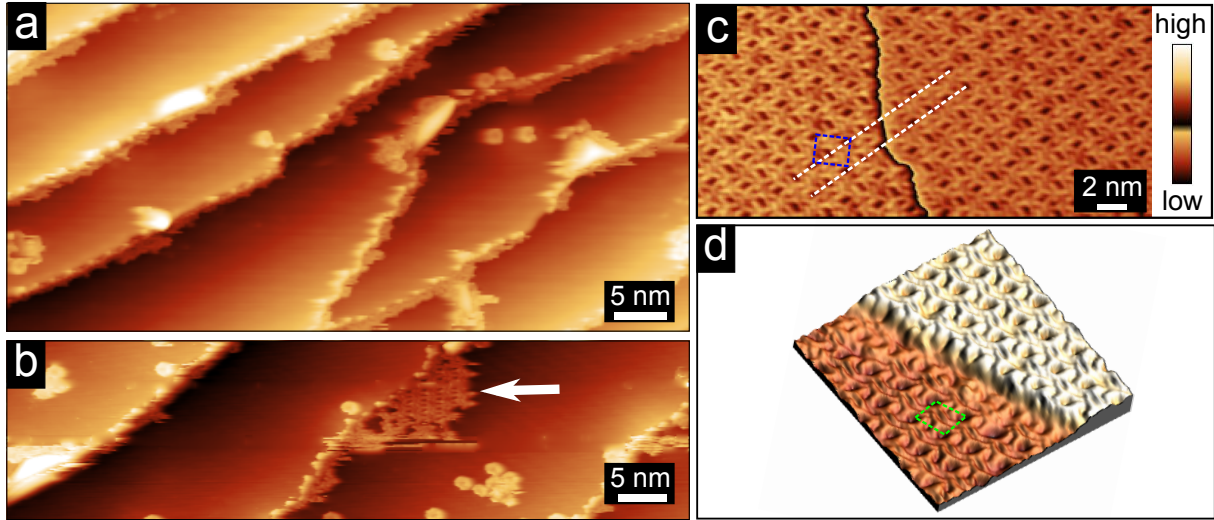


Figure 2: Early stage of growth of TBB on Gr/Ir(111). STM topographs recorded after deposition of (a) 0.05 monolayer (ML) and (b) 0.2 ML of TBB. The white arrow in (b) points at a self-assembled nanoisland. (c) STM topograph of 1ML-thick nanoisland of molecules organized in the 4MOL phase. White dashed lines highlight the continuity of the molecular lattice across the Gr/Ir step edge. (d) 3D rendering of an STM topograph recorded on a 1ML-thick molecular nanoisland of the 2MOL phase. Blue and green rhombuses in (c) and (d) outline the unit cells of the 4MOL and 2MOL phases respectively. Parameters are: (a) ($65 \times 59 \text{ nm}^2$, $U_T = 2.22 \text{ V}$; $I_T = 20 \text{ pA}$), (b) ($70 \times 56 \text{ nm}^2$, $U_T = 2.22 \text{ V}$; $I_T = 40 \text{ pA}$), (c) ($17 \times 11 \text{ nm}^2$, $U_T = 2.22 \text{ V}$; $I_T = 0.25 \text{ nA}$) and (d) ($10 \times 10 \text{ nm}^2$, $U_T = 2.22 \text{ V}$; $I_T = 0.09 \text{ nA}$).

Molecular packings

In the next paragraph, we will discuss the occurrence and the molecular packing of the two TBB polymorphs on graphene. For each polymorph, three different domains rotated from another by 120° are observed, in good accordance with the underlying 3-fold symmetry of the graphene lattice. The two phases are formed in extended domains in the surface together with nanoislands composed of the two coexisting phases as shown in Fig. 3(a). On this STM topograph, the two polymorphs are visible and form three domains separated by two domain boundaries highlighted with dashed lines.

Submolecular resolution allowed us to identify adsorbed molecules as intact TBB molecules since under specific tunneling conditions such as in Fig. 3(a) and Fig. 4(a,b): carbon rings and bright protrusions at the extremity of phenyl arms corresponding to bromine atoms are

clearly visible.

As a consequence, a simple ball and stick model of the molecule can be laid over the STM image of Fig. 3(a). One can readily notice that the building block of the supramolecular network is a molecular dimer as schematically drawn in Fig. 3(b). We will show in the following that dimers are stabilized with C-Br \cdots Br and Br \cdots H bonds. This dimer can be characterized by the distance between the two central carbon rings C (Fig. 1(d)) together with the relative angle between the γ directions made by opposite bromophenyl arms. The unit cells shown in Fig. 3(a) of the 2MOL (green full line) and 4MOL (blue dashed line) phases host two and four TBB molecules respectively. The two phases are oriented such that the diagonal of the 2MOL unit cell corresponds to the shortest side of the 4MOL unit cell.

The determination of the orientation of the supramolecular network with respect to the substrate was not possible neither from LEED patterns nor STM topographs. Indeed, molecules are damaged under the electron beam probably due to electron-induced dissociation. Moreover, the set of tunneling parameters (I_T , U_T) needed to observe the molecular network and the graphene moiré pattern are very different making impossible the simultaneous observation of the TBB-covered and uncovered Gr/Ir surface. However, the two-dimensional Fourier Fast Transforms (2D FFT) of an STM topograph recorded on the self-assembly revealed, under certain tunneling conditions, both Gr/Ir moiré and molecular reciprocal unit cells (see in Supporting Information, Fig. S6) . A 2D FFT of the STM image of a polymorph can thus extract with great accuracy the information about the unit cell vectors and SAMN orientation with respect to the moiré superstructure and the graphene lattice, by extension. Indeed, this method allows to get rid of the well-known experimental artifacts related to STM such as creep distortion, temperature drift or distance calibration. An example of a calculated 2D FFT of an STM topograph recorded on the 2MOL arrangement is given in Fig. 3(c). The six inner spots linked with white dotted lines forming an hexagon correspond to the moiré superlattice. The outer spots linked with pink dotted lines forming a rhombus are related to the 2MOL SAMN. On the basis of the superperiodicity of the moiré unit

cell, we could rigorously lattice-correct the STM topograph. Then, the unit cells vectors could be extracted: \vec{a}_2 and \vec{b}_2 of the 2MOL network are such that $\|\vec{a}_2\| = 1.51 \pm 0.05$ nm, $\|\vec{b}_2\| = 1.93 \pm 0.06$ nm and $(\vec{a}_2, \vec{b}_2) = 103 \pm 2^\circ$. The 4MOL unit cell is rectangular and characterized by \vec{a}_4 and \vec{b}_4 such that $\|\vec{a}_4\| = 2.53 \pm 0.08$ nm, $\|\vec{b}_4\| = 2.22 \pm 0.07$ nm and $(\vec{a}_4, \vec{b}_4) = 89 \pm 2^\circ$. The vectors \vec{a}_2 and \vec{a}_4 make an angle of 4° with the zigzag $\langle \bar{1}210 \rangle$ direction of graphene. The models of the lattice vectors of the two TBB SAMN are illustrated in Fig. 3(d). The molecular density can thus be calculated and is equal to about 0.7 molecule per nm² for each phase.

Starting from the abovementioned lattice vectors, DFT calculations were performed to obtain the optimized structures of the TBB networks. The graphene-molecule interaction was taken into account through a starting block made of the optimized structure of a single TBB molecule adsorbed on pristine graphene as depicted in Supporting Information (Fig. S7). DFT calculations of the self-assembly on graphene couldn't be carried out considering the incommensurability with the substrate that does not allow for the use of a tractable calculation cell. Nevertheless, considering the substrate through the use of the abovementioned starting block is satisfactory since it leads to computed structures in excellent agreement with experimental measurements.

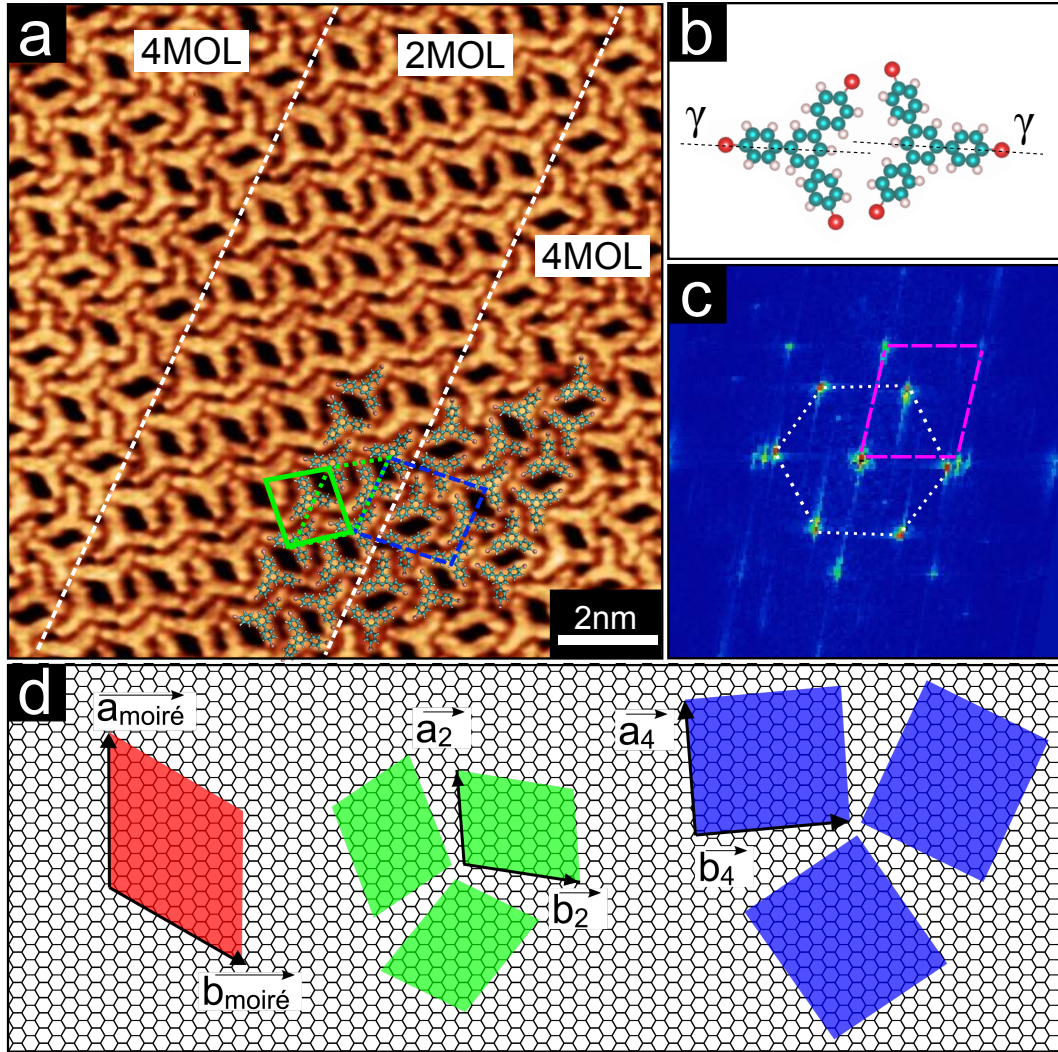


Figure 3: (a) STM topograph of TBB on Gr/Ir(111) showing molecular domains and domain boundaries between the two TBB polymorphs that are delimited by white dashed lines. Full line green and dashed line blue rhombuses outline the unit cells of the 2MOL and 4MOL polymorphs respectively. Ball-and-stick model of molecules are overlaid ($14 \times 14 \text{ nm}^2$, $U_T = 2.22 \text{ V}$; $I_T = 80 \text{ pA}$). (b) Scheme of the TBB dimer building block. Carbon atoms are green, bromine atoms red, and hydrogen atoms white. The dimer is characterized by the angle between the two directions γ in dashed lines made by central C rings and bromophenyl arms and the distance between C bromophenyl rings. (c) 2D Fast Fourier Transform of an STM topograph recorded on the 2MOL arrangement. White dotted and pink dashed lines link spots originating from graphene moiré and molecular cell respectively. (d) Structural model of the growth of TBB on Gr/Ir(111) extracted from the 2D Fast Fourier Transforms of STM images taken on the 2MOL and 4MOL arrangements. Red, green and blue rhombuses represent the unit cells of the graphene moiré on Ir(111), 2MOL and 4MOL polymorphs respectively. Orientations of the unit cells with respect to the graphene moiré have been respected. A graphene honeycomb lattice corresponding to the red moiré unit cell is overlaid.

Considering these optimized structures allowed us to model the two phases in very good agreement with STM images as shown in Fig. 4(a,b) where DFT calculations have been laid over high-resolution STM topographs recorded on 2MOL and 4MOL phases. The superimposition of the graphene lattice and the two phases according to their respective orientations in Fig. 4(c) reveals that the bromophenyl groups are not perfectly aligned with *zigzag* $\langle \bar{1}210 \rangle$ or *armchair* $\langle 10\bar{1}0 \rangle$ direction. γ directions are rotated by an angle of about 4° with respect to the armchair (zigzag) direction for yellow or black (green) molecules.

The 2MOL phase can be simply described as rows of dimers represented as yellow full and dashed lines stars in Fig. 4(c). The 4MOL phase is composed of alternative rows of two distinct pairs of dimers (black and green stars in Fig. 4(c)). Indeed, black and green dimers are not mirror images: the distance between C-rings and angle between γ directions are different for black and green pairs in the theoretical arrangements. This is experimentally confirmed by high-resolution STM topographs. Moreover, this is made clearly visible in the 3D representations in Fig. 4(d) for which green dimers are flatter than black ones.

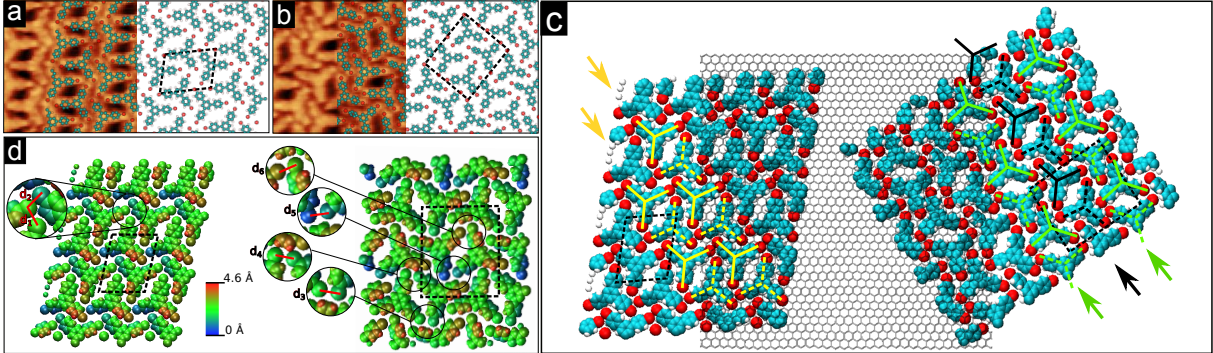


Figure 4: DFT models of TBB networks on Gr/Ir(111) overlaid on an atomically-resolved STM image of the (a) 2MOL and (b) 4MOL polymorph ($5 \times 5 \text{ nm}^2$, $U_T = 2.05 \text{ V}$; $I_T = 175 \text{ pA}$). Rhombuses outline the unit cells of the two polymorphs. (c) Graphene lattice superimposed on DFT models of the 2MOL (left) and the 4MOL (right) polymorphs. (d) DFT calculated structure of TBB SAMNs. Colorscale corresponds to the height (z position) of the atoms. Unit cells are outlined with dotted line.

The 3D representations of the DFT models in Fig. 4(d) help us to understand intermolecular interactions governing the self-assembly process. The nature of the C-Br...Br-C

bond in molecular crystals has only been recently unravelled⁴³ and properties of the halogen bond has been under debate for a long time.¹ One crucial property of the halogen bond is its directionality originating from the electron density of the halogen atom that is anisotropically distributed whenever the atom is covalently bound to another one. It was shown that a higher electron density, where the electrostatic potential is negative forms a belt orthogonal to the covalent bond and a region of lower electron density, where the potential is positive (the so-called σ -hole) forms a cap of depleted electron density in the direction of the covalent bond.^{44,45} We have shown by calculating the electrostatic surface potential (ESP) map that, in the case of TBB, an electron density anisotropy exists as shown in Supporting Information (Fig. S8). Based on these results and recent works,^{1,43} we have retained two criteria for the occurrence of the C-Br...Br-C bond: (i) the distance between bromine atoms has to be smaller than 4.2 Å and it also requires that (ii) $\theta_1 \approx 180^\circ$ and $\theta_2 \approx 90^\circ$ (or, equivalently $\theta_2 \approx 180^\circ$ and $\theta_1 \approx 90^\circ$) such that $|\theta_1 - \theta_2| > 50^\circ$ where θ_1 and θ_2 refer to $\angle C - Br_1 \dots Br_2$ and $\angle C - Br_2 \dots Br_1$ angles. According to these criteria, we have identified two and four C-Br...Br-C intermolecular bonds in the 2MOL and 4MOL phase, respectively (see Tab. 1)

Table 1: Computed interatomic distances (see text and Fig. 4(d) for labels) of the TBB molecular network.

#	d(Å)	$\theta_1(^\circ)$	$\theta_2(^\circ)$	$ \theta_1 - \theta_2 (^\circ)$
1	3.94	92	142	50
2	3.69	90	152	62
3	3.84	88	154	66
4	4.06	85	157	72
5	3.96	92	149	57
6	3.84	94	148	54

Inside the 2MOL packing, dimers are stabilized via one C-Br...Br contact (distance d1 in Fig. 4(d) and see Tab. 1) and neighboring dimers are binded through Br...Br bonds as highlighted by a circle in the figure (distance d2) and C-Br...H bonds. Each type of dimers in the 4MOL packing is stabilized by two C-Br...Br bond (d3 to d6) and inter-rows interactions are of C-Br...H character.

In order to fully characterize the molecule/graphene interface, we have investigated by means of DFT calculations the geometrical conformation of the TBB on Gr/Ir and compared it with pristine graphene and the free molecule. As a result, a strong flattening of the TBB molecule is obtained when adsorbed on Gr/Ir(111) such that one of bromophenyl arms lies totally flat (dihedral angle equals to 0°) (see Tab. 2 and in Supporting Information, Fig. S7(c)). This flattening of TBB on Gr/Ir is as strong as on pristine graphene (see in Supporting Information, Fig. S7(b)) suggesting that the carbon layer is solely responsible for this effect. As a conclusion, TBB gets flat as a consequence of π - π interactions with the graphene layer overcoming repulsive interactions between hydrogen atoms.

Table 2: Dihedral angles of TBB for adsorption situations described in Supporting Information (Fig. S7)

# bromophenyl arm	Gaseous phase	on pristine Gr	on Gr/Ir(111)
1	39°	0°	1°
2	40°	17°	18°
3	39°	9°	12°

In order to fully understand the coexistence of the two polymorphs, binding energy calculations have been performed. First, the binding energies of the two free-standing polymorphs have been calculated and are equal to -0.52 eV. In order to estimate the influence of the substrate, we have calculated the binding energy of a single TBB molecule adsorbed on Gr/Ir on FCC and ATOP regions as defined in Fig. 1(b) and for two equilibrium orientations of the molecule called *staggered* and *eclipsed* where the γ directions are either parallel to zigzag $\langle 1\bar{2}10 \rangle$ or armchair $\langle 10\bar{1}0 \rangle$ directions of the graphene layer (see in Supporting Information, Fig. S7(b) for eclipsed geometry), respectively. We show that the binding energies for all these configurations are equal (-2.5 ± 0.1 eV). The first conclusion to draw is that there is no preferential adsorption site *i.e.* the graphene moiré has no influence on the molecular packing. The second point is that both orientations are energetically equivalent. One can understand that from the substrate point of view, positioning black/yellow or green dimers as depicted in Fig. 4(c) would cost the same amount of energy. These results demonstrate that

the 4MOL phase is energetically equivalent to the 2MOL phase explaining the coexistence of the two polymorphs.

The 2MOL and 4MOL phases of TBB are strongly distinct from the single phase previously obtained on HOPG.³⁷ Generally, it is not straightforward to predict whether the molecular packings will be identical or distinct than on HOPG due to the fact that the behaviour of molecules depends on both molecule-substrate and intermolecular interactions. The difference between the two substrates lies in the interaction of the upmost carbon layer with the neighboring layer (carbon in the case of HOPG and Ir in the case of Gr/Ir). HOPG is composed of stacked graphene layers with interplanar Van der Waals forces whereas Gr/Ir is made of one single layer graphene interacting with a metallic substrate. *A priori*, we would have expected a weak influence of the metallic layer and therefore same arrangements for both substrates since Ir presents a weak interaction with the graphene sheet.^{46,47} In the case of Co and Fe metallated phthalocyanines, a square lattice is observed on Gr/Ir as well as on HOPG despite a unit cell slightly contracted. Nevertheless, additional phases are observed in the case of HOPG. In our case, although the interaction with the underlying layers is weak like in HOPG, the arrangements of TBB are different than on HOPG. That shows that even minute modifications of the interface can have a non negligible influence on the molecular packings.

The building block composed of a molecular dimer has also been observed in other systems such as in the bulk compound,⁴⁸ in SAMNs on HOPG as discussed above,³⁷ on Au(111)⁴² and for related molecules such as 1,3,5-tris(4-iodophenyl)-benzene (TIB) on HOPG³⁸ where bromine is substituted by iodine and 2,4,6-tris(4-bromophenyl)-1,3,5-triazine (TBT) on Au(111) for which the benzene ring has been replaced by a triazine core.³⁶ Although the building block is the same, the 4MOL phase has never been reported before. Concerning the 2MOL phase, one can find packing similarities with the phase labeled "phase I" in reference⁴² of TBB on Au(111) and the one called " *α phase*" of TBT at the liquid/Au(111) interface.³⁶ However, in both cases, the two molecules fit in larger unit cells showing once

again the non negligible influence of the substrate on the molecular arrangement. Larger distances between molecules can lead to a different bonding scheme playing a role in properties such as reactivity. Moreover, other coexisting phases which are not observed in our case are present on the Au(111) surface and are imposed by the so-called herringbone surface reconstruction³⁶ and will surely modify the overall properties of the molecule/substrate interface.

Electronic properties

Finally, we have investigated the electronic properties by LT-STs recorded on bare and TBB-covered Gr/Ir surface and compared those results with calculated PDOS for free and adsorbed molecules on different Gr/Ir site (ATOP,FCC) and different orientations with respect to the substrate (eclipsed or staggered). Experimental dI/dV spectra were averaged over several unit cells of the two polymorphs. The dI/dV spectrum in Fig. 5(a) of the uncovered Gr/Ir surface (full red line) reveals one single feature at about -0.280 eV that is attributed to the Ir surface state that is known to be preserved upon graphene adsorption.⁴⁹ The dI/dV spectrum recorded on the 4MOL SAMN is shown as a dotted line in Fig. 5(a). Note that the one obtained on the 2MOL phase is identical (not shown here). In the range of ± 1 eV, the conductance is dominated by the local density of states of the substrate. Above this range, extra features that can be attributed to molecular states are observed. The conductance starts to increase faster than the Gr/Ir one below -1.1 eV and above $+1.6$ eV leading to a HOMO-LUMO gap of about 2.7 eV.

The observation that dI/dV spectra are identical for both polymorphs is in good agreement with the fact that the projected density of states (PDOS) of TBB on Gr/Ir varies only slightly with the adsorption site or the orientation of the molecule as shown in Supporting Information (Fig. S9 and Fig. S10). In order to measure the impact of the underlying Ir substrate upon the electronic properties of the system, we have compared the calculated PDOS of TBB adsorbed on Gr/Ir (Fig. 5(b)) and on pristine Gr (Fig. 5(c)). As a result,

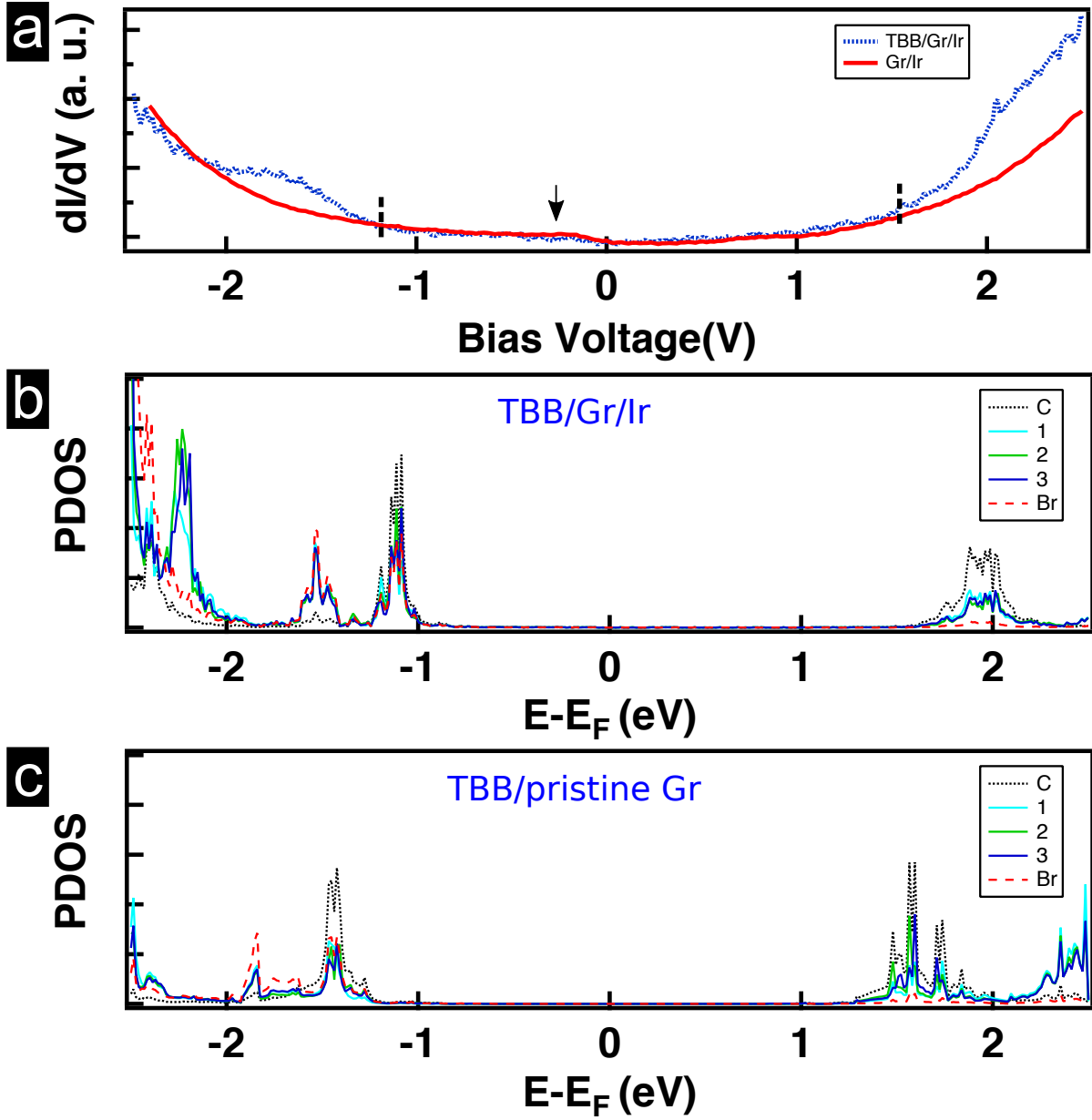


Figure 5: (a) Spatially averaged tunneling spectra recorded over Gr/Ir and on a monolayer of 4MOL polymorph on Gr/Ir(111). The arrow points at the Gr/Ir surface state. Projected densities of states (PDOS) of one single TBB molecule adsorbed (b) on a FCC site of Gr/Ir(111) and (c) on pristine Gr. PDOS are projected on different rings 1, 2, 3 and C as labelled in Fig. 1(d) and on bromine atoms.

the addition of Ir layers leads to a rigid shift of the HOMO and LUMO states leaving the HOMO-LUMO gap unchanged. This can be simply explained by the fact that Ir induces a charge transfer resulting in a p-doped graphene as obtained theoretically here and exper-

imentally.^{46,47} The measured HOMO-LUMO gap of 2.7 eV is much smaller than the one of a single molecule in gas-phase for which our DFT calculations gives a value of 3.5 eV (Note that, it is well known that DFT calculations based on semi-local exchange correlation functional severely underestimate HOMO-LUMO gaps.⁵⁰). This comparison highlights the fact that the presence of the substrate has a non negligible influence on the electronic properties of the molecule. The experimental value is in good agreement with our calculated value of 2.8 eV of TBB on pristine Gr and Gr/Ir (HOMO-LUMO gaps are summarized in Tab.3). We obtain theoretically for TBB inside a 4MOL SAMN without any substrate, a HOMO-LUMO gap higher than 3 eV and an electronic state close to the Fermi level (see in Supporting Information Fig. S11). These two last features are not in agreement with our STS measurements for which an energy gap between the LUMO and HOMO states of 2.7 eV has been measured and no conductance peak at zero bias (Fermi energy) is observed. Once again, this leads to the conclusion that the substrate is responsible for a drastic change in the electronic states. On the contrary, we obtain a very good agreement when considering the TBB molecule adsorbed on pristine graphene (see in Supporting Information, Fig. S11(b)) or Gr/Ir (Fig. 5(b)) regardless the adsorption site or the orientation of the molecule with respect to the graphene underlayer (see in Supporting Information Fig. S9 and Fig. S10). According to the corresponding PDOS, these states are mainly of p_z character (see in Supporting Information Fig. S12). Experimental determination of HOMO and LUMO energies or HOMO-LUMO gaps of adsorbed TBB are lacking in the literature and do not allow for a comparative study with other substrate. Nevertheless, a HOMO-LUMO gap of 1.4 eV of TBB adsorbed on boron-doped Si (111) has been calculated.⁵¹ It is smaller than the one obtained in our work for TBB on graphene leading to the conclusion that the Gr/Ir provides weaker molecular-substrate interactions than SiB.

Table 3: Experimental and computed HOMO-LUMO gaps of the TBB adsorbed on X/(Y) where X is the adsorption site and Y the surface. The symbol ./ is used when the adsorption site is not specified.

Experimental	
./(Gr/Ir)	2.7 eV
DFT	
gas-phase	3.5 eV
./(pristine Gr)	2.8 eV
FCC/(Gr/Ir)	2.8 eV
TOP/(Gr/Ir)	2.8 eV

Conclusions and Perspectives

In summary, low-temperature scanning tunneling microscopy (LT-STM) and density functional theory (DFT) were used to investigate the structural formation of 1,3,5-tri(4'-bromophenyl)benzene (TBB) self-assembled monolayers on epitaxial graphene on Ir(111). The molecules adsorb on the Gr/Ir(111) substrate at room temperature and give rise to two distinct and coexisting well-ordered phases. Submolecular resolution STM topographs show that the molecular building block of these packings is a pair of TBB molecules. DFT calculations reveal that in both phases, intermolecular interactions are of C-Br \cdots Br and C-Br \cdots H type. The advantages of using Gr/Ir as a support lies in the obtention of highly-ordered molecular arrangements unperturbed by surface step edges. The high interfacial uniformity is a key criterion to optimize operation and performances of organic devices. Moreover, the presence of the graphene moiré pattern induced by the presence of the Ir layer helped us to determine the molecular lattices with great accuracy. In addition, we show that the TBB HOMO-LUMO gap is highly reduced when adsorbed on graphene revealing the non negligible interaction with the substrate. The presence of Ir below graphene induces a charge transfer from graphene resulting in a rigid shift of the HOMO-LUMO states compared to pristine graphene. Nevertheless, Ir has only little influence on the adsorption geometry of the molecule. DFT reveals that the molecule flattens on graphene and that this flattening is governed by π - π interactions. As a perspective, more systematic investigations such as

the influence of the underlying metal using intercalation for example or the dependence of the halogen atoms on the molecular arrangements are now required. In addition, molecules with different symmetries and number of halogen termination could be used to grow novel molecular architectures. Considering the importance of halogen···halogen interactions in the growth of molecular crystals and the fact that graphene is a promising candidate for future electronic devices, this work opens up new routes for the fabrication of next-generation organic devices.

Experimental section

DFT calculations. In the present study, we have investigated using Density Functional Theory (DFT) as implemented in the Vienna *ab initio* simulation package (VASP),^{52–55} the structural and energetic properties of the two main self assembly TBB structures on Graphene@Ir(111). The corrugated Graphene@Ir(111) structure was modeled with a (10×10) Graphene structure over a (9×9) Ir(111) surface cells with 4 atomic layers, as proposed in different recent studies.^{56–58} A (10×10) graphene cell was used for the study of the TBB molecule on the free standing graphene. As usual in this type of calculations, we have applied a supercell approach, with a vacuum region of more than 20 Å to avoid interaction between periodic images in the z direction. To obtain the reference energy and the optimized structure of a single TBB molecule in gas phase we have used the same cell as the free standing graphene layer. It has a lattice constant equal to $a_0 = 2.46$ Å, close to the experimentally obtained value (2.459 Å) for a graphite at low temperatures.⁵⁹

Ions cores were modeled with projector augmented wave (PAW) pseudopotentials.⁶⁰ The 2s and 2p states of carbon, 1s state of hydrogen and 4s and 4p states of bromine were treated explicitly in the valence. The plane-wave basis set cutoff energy is set to 400 eV with a Gaussian smearing method of 0.1 eV width, in order to assure well converged total energy and force values. To include van der Waals interactions in our calculations, we have used

the optB86b-vdW scheme.^{61,62} This particular choice of exchange-correlation functional is based on several previous works.⁶³⁻⁶⁷ All the atoms were allowed to relax until the maximum of all forces acting on them became smaller than $0.02 \text{ eV.}\text{\AA}^{-1}$. The k-point sampling was always based on a Γ -centered grid for all types of calculations. We have used, to optimize the structures, a single k-point calculation for the TBB molecule, a $(4 \times 4 \times 1)$ grid for the TBB-graphene system, a $(4 \times 4 \times 1)$ grid for 2-TBB, a $(3 \times 3 \times 1)$ grid for 4-TBB case, when a $(2 \times 2 \times 1)$ grid for the single TBB on graphene@Ir(111) system was used. To determine the density of states (DOS), the tetrahedron integration method with Blöchl corrections⁶⁸ was used, with a $(6 \times 6 \times 1)$ grid for the TBB-graphene and for the TBB on Graphene@Ir(111), a $(7 \times 7 \times 1)$ grid for 2MOL and a $(5 \times 5 \times 1)$ grid for 4MOL.

We have compared the energy stability of two structures, 2MOL and 4MOL, via the cohesion energy E_{coh} of n TBB molecules. This energy can be calculated from the following equation :

$$E_{\text{coh}} = E_{n\text{MOL}} - nE_{\text{TBB}}, \quad (1)$$

where $E_{n\text{MOL}}$ is the total energy of $n\text{MOL}$ system and E_{TBB} is the energy of single free TBB molecule.

Molecule and substrate preparation. The experiments were carried out in an ultra high vacuum system with a base pressure of 1×10^{-10} mbar equipped with an low-temperature STM Omicron. The Ir(111) single crystal was cleaned by repeated cycles of Ar^+ sputtering at an energy of 1.5 keV followed by a flash annealing to 1100 K. An ordered graphene monolayer (ML) was prepared by cracking on Ir(111) held at 1100 K under a propene pressure of 3×10^{-7} mbar for 5 min. 1,3,5-tri(4'-bromophenyl)-benzene was purchased from Aldrich and then purified by column chromatography on silica gel. Then, the molecules were sublimated using a Knudsen evaporation cell onto a substrate held at room temperature.

STM/STS experiments. All microscopy and spectroscopy measurements were performed at 77 K. The STM images were recorded at a tunneling current I_T and a bias voltage U_T where its sign corresponds to the voltage applied to the sample. STS spectra were ac-

quired with a PtIr tip and a lock-in current detection (bias modulation of 70 mV, frequency 1100 Hz) , in open feedback loop conditions.

Acknowledgment

D. Tristant thanks the Midi-Pyrénées Région and the PRES Université de Toulouse for PhD funding. I. Gerber and D. Tristant also acknowledge the Calcul en Midi-Pyrénées initiative-CALMIP (Project p0812) for allocations of computer time. Part of this work was also performed using HPC resources from GENCI-IDRIS and GENCI-CINES (Project x2015096649). I. Gerber thanks CNRS for financial support.

Supporting Information available

Raw STM images showing both graphene moiré and molecular lattices. Projected densities of states of one single TBB molecule adsorbed on various surfaces and geometries. Dihedral angles of TBB for various adsorption geometries. Computed interatomic distances of the TBB molecular network. Experimental and computed HOMO-LUMO gaps of the adsorbed TBB. Optimized geometry of TBB calculated by DFT. Molecular ESP map of TBB in gas phase.

References

1. Cavallo, G.; Metrangolo, P.; Milani, R.; Pilati, T.; Priimagi, A.; Resnati, G.; Terraneo, G. The Halogen Bond. Chem. Rev. **2016**, *116*, 2478–2601.
2. Griessl, S.; Lackinger, M.; Edelwirth, M.; Hietschold, M.; Heckl, W. M. Self-Assembled Two-Dimensional Molecular Host-Guest Architectures From Trimesic Acid. Single Mol. **2002**, *3*, 25–31.
3. Lei, S.; Wang, C.; S.X.Yin.; Wang, H.; Xi, F. Surface Stabilized Porphyrin and Phthalo-

- cyanine Two-Dimensional Network Connected by Hydrogen Bonds. J. Phys. Chem. B **2001**, 105, 10838–10841.
4. Yokoyama, T.; Yokoyama, S.; Kamikado, T.; Okuno, Y.; Mashiko, S. Selective Assembly on a Surface of Supramolecular Aggregates with Controlled Size and Shape. Nature **2001**, 413, 619–621.
 5. Wei, Y.; Tong, W.; Zimmt, M. B. Self-Assembly of Patterned Monolayers with Nanometer Features: Molecular Selection Based on Dipole Interactions and Chain Length. J. Am. Chem. Soc. **2008**, 130, 3399–3405.
 6. Lingensfelder, M. A.; Spillmann, H.; Dmitriev, A.; Stepanow, S.; Lin, N.; Barth, J. V.; Kern, K. Towards Surface-Supported Supramolecular Architectures: Tailored Coordination Assembly of 1,4-Benzenedicarboxylate and Fe on Cu(100). Chem. Eur. J **2007**, 10, 1913–1919.
 7. Stepanow, S.; Lin, N.; Payer, D.; Schlickum, U.; Klappenberger, F.; Zoppellaro, G.; Ruben, M.; Brune, H.; Barth, J. V.; Kern, K. Surface-Assisted Assembly of 2D Metal-Organic Networks That Exhibit Unusual Threefold Coordination Symmetry. Angew. Chem. Int. Ed. **2007**, 46, 710–713.
 8. Giovannantonio, M. D.; Garah, M. E.; Lipton-Duffin, J.; Meunier, V.; Cardenas, L.; Revurat, Y. F.; Cossaro, A.; Verdini, A.; Perepichka, D. F.; Rosei, F. et al. Insight into Organometallic Intermediate and Its Evolution to Covalent Bonding in Surface-Confined Ullmann Polymerization. ACS Nano **2013**, 7, 8190–8198.
 9. Qiu, X.; Wang, C.; Zeng, Q.; Xu, B.; Yin, S.; Wang, H.; Xu, S.; Bai, C. Alkane-Assisted Adsorption and Assembly of Phthalocyanines and Porphyrins. J. Am. Chem. Soc. **2000**, 122, 5550–5556.
 10. Nath, K. G.; Ivasenko, O.; MacLeod, J. M.; Miwa, J. A.; Wuest, J. D.; Nanci, A.;

- Perepichka, D. F.; Rosei, F. Crystal Engineering in Two Dimensions: An Approach to Molecular Nanopatterning. J. Phys. Chem. C **2007**, 111, 16996–17007.
11. ger, D. B.; Kreher, D.; Mathevet, F.; Attias, A.-J.; Schull, G.; Huard, A.; Douillard, L.; Fiorini-Debuischert, C.; Charra, F. Surface Noncovalent Bonding for Rational Design of Hierarchical Molecular Self-Assemblies. Angew. Chem. Int. Ed. **2007**, 46, 7404–7407.
 12. Grimme, S. Do Special Noncovalent pi-pi Stacking Interactions Really Exist? Angew. Chem. Int. Ed. **2008**, 47, 3430–3434.
 13. MacLeod, J. M.; Rosei, F. Molecular Self-assembly on Graphene. Small **2014**, 10, 1038–1049.
 14. Marchini, S.; Günther, S.; Wintterlin, J. Scanning Tunneling Microscopy of Graphene on Ru(0001). Phys. Rev. B **2007**, 76, 075429.
 15. N'Diaye, A. T.; Coraux, J.; Plasa, T. N.; Busse, C.; Michely, T. Structure of Epitaxial Graphene on Ir(111). New J. Phys. **2008**, 10, 043033.
 16. Sicot, M.; Bouvron, S.; Zander, O.; Rudiger, U.; Dedkov, Y. S.; Fonin, M. Nucleation and Growth of Nickel Nanoclusters on Graphene Moiré on Rh(111). Appl. Phys. Lett. **2010**, 96, 093115.
 17. Land, T. A.; Michely, T.; Behm, R. J.; Hemminger, J. C. STM Investigation of Single Layer Graphite Structures Produced on Pt (111) by Hydrocarbon Decomposition. Surf. Sci. **1992**, 264, 261–270.
 18. Cai, Y.; Zhang, H.; Song, J.; Zhang, Y.; Bao, S.; He, P. Adsorption Properties of CoPc Molecule on Epitaxial Graphene/Ru(0001). Appl. Surf. Sci. **2015**, 327, 517–522.
 19. Mao, J.; Zhang, H.; Jiang, Y.; Pan, Y.; Gao, M.; Xiao, W.; Gao, H. J. Tunability of Supramolecular Kagome Lattices of Magnetic Phthalocyanines Using Graphene-Based Moiré Patterns as Templates. J. Am. Chem. Soc. **2009**, 131, 14136–14137.

20. Scheffler, M.; Smykalla, L.; Baumann, D.; Schlegel, R.; Hänke, T.; M. Toader; Büchner, B.; Hietschold, M.; Hess, C. Structural Study of Monolayer Cobalt Phthalocyanine Adsorbed on Graphite. Surf. Sci. **2013**, 608, 55–60.
21. Åhlund, J.; Schnadt, J.; Nilson, K.; Göthelid, E.; Schiessling, J.; Besenbacher, F.; Mårtensson, N.; Puglia, C. The Adsorption of Iron Phthalocyanine on Graphite: A Scanning Tunnelling Microscopy Study. Surf. Sci. **2007**, 601, 3661–3667.
22. Yang, K.; Xiao, W. D.; Jiang, Y. H.; Zhang, H. G.; Liu, L. W.; Mao, J. H.; Zhou, H. T.; Du, S. X.; Gao, H. J. Molecule-Substrate Coupling between Metal Phthalocyanines and Epitaxial Graphene Grown on Ru(0001) and Pt(111). J. Phys. Chem. C **2012**, 116, 14052–14056.
23. Shikin, A. M.; Prudnikova, G. V.; Adamchuk, V. K.; Moresco, F.; Rieder, K.-H. Surface Intercalation of Gold Underneath a Graphite Monolayer on Ni(111) Studied by Angle-Resolved Photoemission and High-Resolution Electron-Energy-Loss Spectroscopy. Phys. Rev. B **2000**, 62, 13202.
24. Dedkov, Y. S.; Shikin, A. M.; Adamchuk, V. K.; Molodtsov, S. L.; Laubschat, C.; Bauer, A.; Kaindl, G. Intercalation of Copper Underneath a Monolayer of Graphite on Ni(111). Phys. Rev. B **2001**, 64, 035405.
25. Varykhalov, A.; Sánchez-Barriga, J.; Shikin, A. M.; Biswas, C.; Vescovo, E.; Rybkin, A.; Marchenko, D.; Rader, O. Surface Intercalation of Gold Underneath a Graphite Monolayer on Ni(111) Studied by Angle-Resolved Photoemission and High-Resolution Electron-Energy-Loss Spectroscopy. Phys. Rev. B **2000**, 62, 13202.
26. Enderlein, C.; Kim, Y. S.; Bostwick, A.; Rotenberg, E.; Horn, K. The Formation of an Energy Gap in Graphene on Ruthenium by Controlling the Interface. New J. Phys **2010**, 12, 033014.

27. Sutter, P.; Sadowski, J. T.; Sutter, E. A. Chemistry under Cover: Tuning Metal-Graphene Interaction by Reactive Intercalation. J. Am. Chem. Soc. **2010**, 132, 8175–8179.
28. Rutkov, E. V.; Gall, N. R. Intercalation of Graphene Films on Metals with Atoms and Molecules, Physics and Applications of Graphene - Experiments. Dr. Sergey Mikhailov (Ed.), InTech
29. Sicot, M.; Leicht, P.; Zusan, A.; Ole Zander, M. W.; Dedkov, Y. S.; Horn, K. Size-Selected Epitaxial Nanoislands Underneath Graphene Moiré on Rh(111). ACS Nano **2012**, 6, 151–158.
30. Sicot, M.; Fagot-Revurat, Y.; Vasseur, G.; Kierren, B.; Malterre, D. Copper Intercalation at the Interface of Graphene and Ir(111) Studied by Scanning Tunneling Microscopy. Appl. Phys. Lett. **2014**, 105, 191603.
31. Bazarnik, M.; Brede, J.; Decker, R.; Wiesendanger, R. Tailoring Molecular Self-Assembly of Magnetic Phthalocyanine Molecules on Fe- and Co-intercalated Graphene. ACS Nano **2013**, 7, 11341–11349.
32. Schumacher, S.; Wehling, T. O.; Lazić, P.; Runte, S.; rster, D. F. F.; Busse, C.; Petrović, M.; Kralj, M.; Blügel, S.; Atodiresei, N. et al. The Backside of Graphene: Manipulating Adsorption by Intercalation. Nano Lett. **2013**, 13, 5013–5019.
33. Coraux, J.; N'Diaye, A. T.; Busse, C.; Michely, T. Structural Coherency of Graphene on Ir(111). Nano Lett. **2008**, 8, 565–570.
34. Sutter, P. W.; Flege, J.-I.; Sutter, E. A. Epitaxial Graphene on Ruthenium. Nat. Mater. **2008**, 7, 406–411.
35. Hämäläinen, S. K.; Stepanova, M.; Drost, R.; Liljeroth, P.; Lahtinen, J.; Sainio, J.

- Self-Assembly of Cobalt-Phthalocyanine Molecules on Epitaxial Graphene on Ir(111). J. Phys. Chem. C **2012**, *116*, 20433–20437.
36. Gatti, R.; MacLeod, J. M.; Lipton-Duffin, J. A.; Moiseev, A. G.; Perepichka, D. F.; Rosei, F. Substrate, Molecular Structure, and Solvent Effects in 2D Self-Assembly via Hydrogen and Halogen Bonding. J. Phys. Chem. C **2014**, *118*, 25505–25516.
37. Gutzler, R.; Walch, H.; Eder, G.; Kloft, S.; Heckl, W.; Lackinger, M. Surface mediated synthesis of 2D covalent organic frameworks: 1,3,5-tris(4-bromophenyl)benzene on graphite(001),Cu(111)and Ag(110). Chem. Comm. **2009**, *29*, 4456–4458.
38. Silly, F. Selecting Two-Dimensional Halogen–Halogen Bonded Self-Assembled 1,3,5-Tris(4-iodophenyl)benzene Porous Nanoarchitectures at the Solid–Liquid Interface. J. Phys. Chem. C **2013**, *117*, 20244–20249.
39. Baris, B.; Luzet, V.; Duverger, E.; Sonnet, P.; Palmino, F.; Cherioux, F. Robust and Open Tailored Supramolecular Networks Controlled by the Template Effect of a Silicon Surface. Angew. Chem. Int. Ed. **2011**, *50*, 4094–4098.
40. Walch, H.; Gutzler, R.; Sirtl, T.; Eder, G.; Lackinger, M. Material- and Orientation-Dependent Reactivity for Heterogeneously Catalyzed Carbon-Bromine Bond Homolysis. J. Phys. Chem. C **2010**, *114*, 12604–12609.
41. Blunt, M. O.; Russell, J. C.; Champness, N. R.; Beton, P. H. Templating Molecular Adsorption Using a Covalent Organic Framework. Chem. Commun. **2010**, *46*, 7157–7159.
42. Russell, J. C.; Blunt, M. O.; Garfitt, J. M.; Scurr, D. J.; Alexander, M.; Champness, N. R.; Beton, P. H. Dimerization of Tri(4-bromophenyl)benzene by Aryl-Aryl Coupling from Solution on a Gold Surface. J. Am. Chem. Soc. **2011**, *133*, 4220–4223.

43. Capdevila-Cortada, M.; Novoa, J. J. The Nature of the C–Br...Br–C Intermolecular Interactions Found in Molecular Crystals: a General Theoretical-Database Study. CrystEngComm **2015**, 17, 3354–3365.
44. Murray, J.; Lane, P.; Politzer, P. Expansion of the sigma-Hole Concept. J. Mol. Model. **2009**, 15, 723–729.
45. Politzer, P.; Murray, J. S.; Clark, T. Halogen Bonding and Other sigma-Hole Interactions: A Perspective. Phys. Chem. Chem. Phys. **2013**, 15, 11178–11189.
46. Preobrajenski, A.; Ng, M. L.; Vinogradov, A. S.; rtensson, N. M. Controlling Graphene Corrugation on Lattice-Mismatched Substrates. Phys. Rev. B **2008**, 78, 073401.
47. Pletikosić, I.; Kralj, M.; Pervan, P.; Brako, R.; Coraux, J.; N'Diaye, A. T.; Busse, C.; Michely, T. Dirac Cones and Minigaps for Graphene on Ir(111). Phys. Rev. Lett. **2009**, 102, 056808.
48. Beltran, L. M. C.; Cui, C.; Leung, D. H.; Xu, J.; Hollander, F. J. 1,3,5-Tris(p-bromophenyl)benzene. Acta Crystallogr., Sect. E: Struct. Rep. Online **2002**, 58, o782–o783.
49. Pletikosić, I.; Kralj, M.; Šokčević, D.; Brako, R.; Lazić, P.; Pervan, P. Photoemission and Density Functional Theory Study of Ir(111); Energy Band Gap mapping. J. of Phys.: Condens. Matter **2010**, 22, 135006.
50. Zhang, G.; Musgrave, C. B. Comparison of DFT Methods for Molecular Orbital Eigenvalue Calculations. J. Phys. Chem.A **2007**, 111, 1554–1561.
51. Boukari, K.; Duverger, E.; Sonnet, P. Full DFT-D Description of a Nanoporous Supramolecular Network on a Silicon Surface. J. Chem. Phys. **2013**, 138, 084704–084713.
52. Kresse, G.; Hafner, J. Ab Initio Molecular Dynamics for Liquid Metals. Phys. Rev. B **1993**, 47, 558.

53. Kresse, G.; Hafner, J. Ab Initio Molecular-Dynamics Simulation of the Liquid-Metal-Amorphous-Semiconductor Transition in Germanium. Phys. Rev. B **1994**, 49, 14251.
54. Kresse, G.; Furthmüller, J. Efficient Iterative Schemes for Ab Initio Total-Energy Calculations Using a Plane-Wave Basis Set. Phys. Rev. B **1996**, 54, 11169.
55. Kresse, G.; Furthmüller, J. Efficiency of Ab-Initio Total Energy Calculations for Metals and Semiconductors Using a Plane-Wave Basis Set. Com. Mat. Sci. **1996**, 6, 15–50.
56. Brako, R.; Šokčević, D.; Lazić, P.; Atodiresei, N. Graphene on the Ir(111) Surface: from Van Der Waals to Strong Bonding. New J. Phys **2010**, 12, 113016.
57. Busse, C.; Lazić, P.; Djemour, R.; Coraux, J.; Gerber, T.; Atodiresei, N.; Caciuc, V.; Brako, R.; N'Diaye, A. T.; Blügel, S. et al. Graphene on Ir(111): Physisorption with Chemical Modulation. Phys. Rev. Lett. **2011**, 107, 036101.
58. Vita, H.; Böttcher, S.; Horn, K.; Voloshina, E. N.; Ovcharenko, R. E.; Kampen, T.; Thissen, A.; Dedkov, Y. S. Understanding the Origin of Band Gap Formation in Graphene on Metals: Graphene on Cu/Ir(111). Sci. Rep. **2014**, 4, 5704–5712.
59. Baskin, Y.; Meyer, L. Lattice Constants of Graphite at Low Temperatures. Phys. Rev. **1955**, 100, 544.
60. Blöchl, P. E. Projector Augmented-Wave Method. Phys. Rev. B **1994**, 50, 17953.
61. Klimeš, J.; Bowler, D. R.; Michaelides, A. Chemical Accuracy for the Van Der Waals Density Functional. J. Physics: Condens. Matter **2010**, 22, 022201.
62. Klimeš, J.; Bowler, D. R.; Michaelides, A. Van der Waals Density Functionals Applied to Solids . Phys. Rev. B **2011**, 83, 195131.
63. Tristant, D.; Puech, P.; Gerber, I. C. Theoretical Study of Graphene Doping Mechanism by Iodine Molecules. J. Phys. Chem. C **2015**, 119, 12071–12078.

64. Hu, T.; Gerber, I. C. Theoretical Study of the Interaction of Electron Donor and Acceptor Molecules with Graphene. *J. Phys. Chem. C* **2013**, *117*, 2411–2420.
65. Hu, T.; Gerber, I. C. Band gap Modulation of Bilayer Graphene by Single and Dual Molecular Doping: A van der Waals Density-Functional Study. *Chem. Phys. Lett.* **2014**, *616*, 75–80.
66. Kong, L.; Enders, A.; Rahman, T. S.; Dowben, P. A. Molecular Adsorption on Graphene. *J. Phys.: Condens. Matter* **2014**, *26*, 443001.
67. Tristant, D.; Wang, Y.; Gerber, I.; Monthieux, M.; Pénicaud, A.; Puech, P. Optical Signatures of Bulk and Solutions of KC8 and KC24. *J. Appl. Phys.* **2015**, *118*, 044304.
68. Blöchl, P. E.; Jepsen, O.; Andersen, O. K. Improved Tetrahedron Method for Brillouin-Zone Integrations. *Phys. Rev. B* **1994**, *49*, 16223.

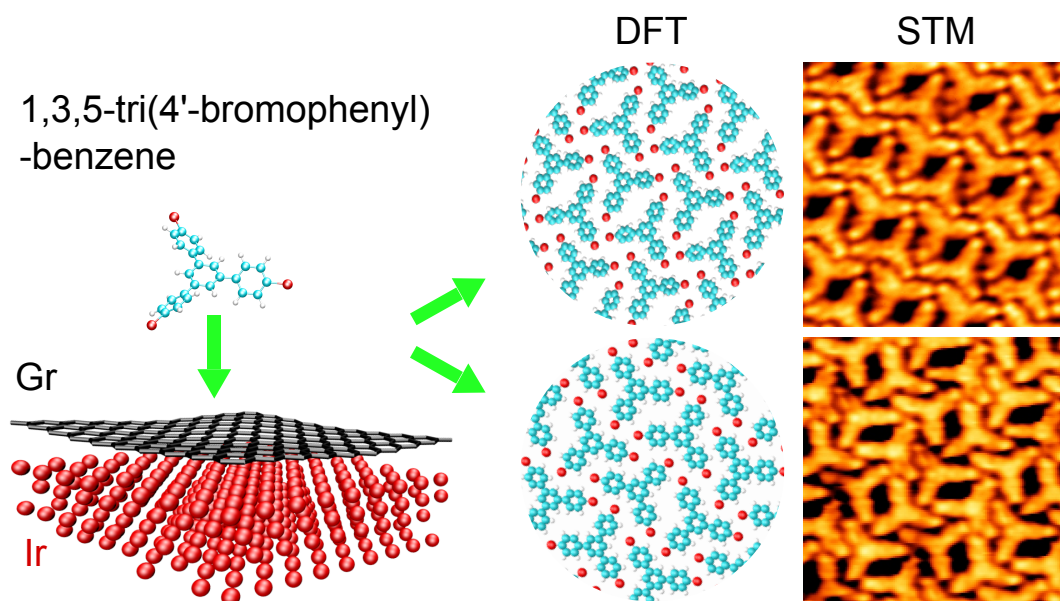


Figure 6: TOC Graphic